

SCTN: Sparse Convolution-Transformer Network for Scene Flow Estimation

Bing Li Cheng Zheng Silvio Giancola Bernard Ghanem
Visual Computing Center, KAUST, Thuwal, Saudi Arabia

Abstract

We propose a novel scene flow estimation approach to capture and infer 3D motions from point clouds. Estimating 3D motions for point clouds is challenging, since a point cloud is unordered and its density is significantly non-uniform. Such unstructured data poses difficulties in matching corresponding points between point clouds, leading to inaccurate flow estimation. We propose a novel architecture named Sparse Convolution-Transformer Network (SCTN) that equips the sparse convolution with the transformer. Specifically, by leveraging the sparse convolution, SCTN transfers irregular point cloud into locally consistent flow features for estimating continuous and consistent motions within an object/local object part. We further propose to explicitly learn point relations using a point transformer module, different from exiting methods. We show that the learned relation-based contextual information is rich and helpful for matching corresponding points, benefiting scene flow estimation. In addition, a novel loss function is proposed to adaptively encourage flow consistency according to feature similarity. Extensive experiments demonstrate that our proposed approach achieves a new state of the art in scene flow estimation. Our approach achieves an error of 0.038 and 0.037 (EPE3D) on FlyingThings3D and KITTI Scene Flow respectively, which significantly outperforms previous methods by large margins.

1. Introduction

Understanding 3D dynamic scenes is critical to many real-world applications such as autonomous driving and robotics. Scene flow is the 3D motion of points in a dynamic scene, which provides low-level information for scene understanding [13, 30, 56]. The estimation of the scene flow can be a building block for more complex applications and tasks such as 3D object detection [47], segmentation [53] and tracking [43]. However, many previous scene flow methods estimate the 3D motion from stereo or RGB-D images. With the increasing popularity of point cloud data, it

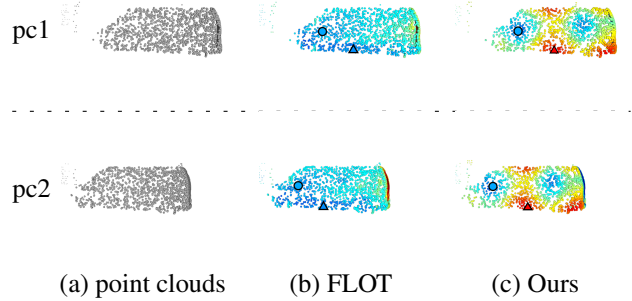


Figure 1. Illustrating the advantage of our SCTN in feature extraction, where first and second rows indicate the two point clouds, (b) and (c) visualize their features extracted by FLOT and our SCTN, respectively. Circles \circ or triangles \triangle in (b)(c) indicate a pair of corresponding points between the point clouds, respectively. \circ and \triangle are not corresponding to each other, however, their features extracted by FLOT are improperly similar, which are less discriminative and would lead to inaccurate predicted flows. In contrast, our SCTN extracts locally consistent while discriminative features.

is desirable to estimate 3D motions directly from 3D point clouds.

Recent methods *e.g.* [28, 30, 40, 58, 62, 65] propose deep neural networks to learn scene flow from point clouds in an end-to-end way, which achieves promising estimation performance. However, estimating scene flow from point clouds is still challenging. In particular, existing methods [30, 40] extract feature for each point by aggregating information from its local neighborhood. However, such extracted features are not discriminative enough to matching corresponding points between point clouds (see Figure 1), leading to inaccurate flow estimation, since the feature extraction of these methods ignore two facts. First, the density of points is significantly non-uniform within a point cloud. It is non-trivial to learn point features that are simultaneously favorable for both points from dense regions and those from sparse regions. Second, due to Lidar and object motions, the density of points within an object often

varies at the temporal dimension, leading that the geometry patterns of corresponding local regions are inconsistent between consecutive point clouds. As a result, extracted features, that are aggregated from only local regions without modeling point relations, is insufficient for scene flow estimation.

Another challenge lies in that most previous methods have to train a model on the synthetic dataset to estimate scene flow for real-world data. However, there exists domain shift between the synthetic dataset and the real-world one. For example, most objects in the synthetic dataset are rigid and undergo rigid motions, while real-world data contains many non-rigid objects whose motions are consistent within local object parts, rather than the whole object. Consequently, the performance of the trained model is degraded when handling real-world data. Yet, most recent work [30, 40, 65] do not explicitly constrain the estimated flows. We would like to enforce the predicted flows in a local region of an object to be *consistent* and *smooth* in 3D space.

In this work, we resort to feature representations and loss functions to estimate accurate scene flow from point clouds. In particular, we explore novel feature representations (information) that would help to infer an accurate and locally consistent scene flows. We therefore propose a Sparse Convolution-Transformer Network (SCTN) which incorporates the merits of dual feature representations provided by our two proposed modules. In particular, to address the issue of spatially non-uniform and temporally varying density of dynamic point clouds, we propose a Voxelization-Interpolation based Feature Extraction (VIFE) module. VIFE extracts features from voxelized point clouds rather than original ones, and then interpolates features for each point, which encourages to generate locally consistent flow features. To further improve discriminability of extracted features from the VIFE module, we propose to additionally model point relations in the feature space, such that extracted features capture important contextual information. Inspired by impressive performance of transformer in object detection tasks [3], we propose a Point Transformer-based Feature Extraction (PTFE) module to explicitly learn point relations based on transformer for capturing complementary information.

In addition, we propose a spatial consistency loss function with a new architecture that equips stop-gradient for training. The loss adaptively controls the flow consistency according to the similarity of point features. Our experiments demonstrate that our method significantly outperforms state-of-the-art approaches on standard scene flow datasets: FlyingThings3D [37] and KITTI Scene Flow [35].

Contributions. Our contributions are fourfold:

1. Instead of designing convolution kernels, our VIFE module leverages simple operators – voxelization and

interpolation for feature extraction, showing such smoothing operator is effective to extract local consistent while discriminative features for scene flow estimation.

2. Our PTFE module shows that explicitly modeling point relations can provide rich contextual information and is helpful for matching corresponding points, benefiting scene flow estimation. We are the first to introduce transformer for scene flow estimation.
3. We propose a new consistency loss equipping stop-gradient-based architecture that helps the model trained on synthetic dataset well adapt to real data, by controlling spatial consistency of estimated flows.
4. We propose a novel network that outperforms the state-of-the-art methods with remarkable margins on both FlyingThings3D and KITTI Scene Flow benchmarks.

2. Related Work

Optical Flow. Optical flow estimation is defined as the task of predicting the pixels motions between consecutive 2D video frames. Optical flow is a fundamental tool for 2D scene understanding, that have been extensively studied in the literature. Traditional methods [1, 2, 17, 45, 63, 68] address the problem of estimating optical flow as an energy minimization problem, that does not require any training data. Dosovitskiy *et al.* [11] proposed a first attempt for an end-to-end model to solve optical flow based on convolution neural network (CNN). Inspired by this work, many CNN-based studies have explored data-driven approaches for optical flow [11, 20–22, 34, 49, 52].

Scene Flow from Stereo and RGB-D Videos. Estimating scene flow from stereo videos have been studied for years [6, 23, 24, 51, 57, 61]. Many works estimate scene flow by jointly estimating stereo matching and optical flow from consecutive stereo frames [38]. Similar to optical flow, traditional methods formulate scene flow estimation as an energy minimization problem [19, 61]. Recent works estimate scene flow from stereo video using neural networks [6]. For example, networks for disparity estimation and optical flow are combined in [23, 33]. Similarly, other works [44, 48] explore scene flow estimation from RGB-D video.

Scene Flow on Point Clouds. Inspired by FlowNet [11], FlowNet3D [30] propose an end-to-end network to estimate 3D scene flow from raw point clouds. Different from traditional methods [10, 55], FlowNet3D [30] is based on PointNet++ [42], and propose a flow embedding layer to aggregate the information from consecutive point clouds and extract scene flow with convolutional layers. FlowNet3D++ [60] improves the accuracy of FlowNet3D by incorporating geometric constraints. HPLFlowNet [15] projects point clouds into permutohedral lattices, and then estimates scene flow using Bilateral Convolutional Layers. Inspired by the successful optical flow method PWC-

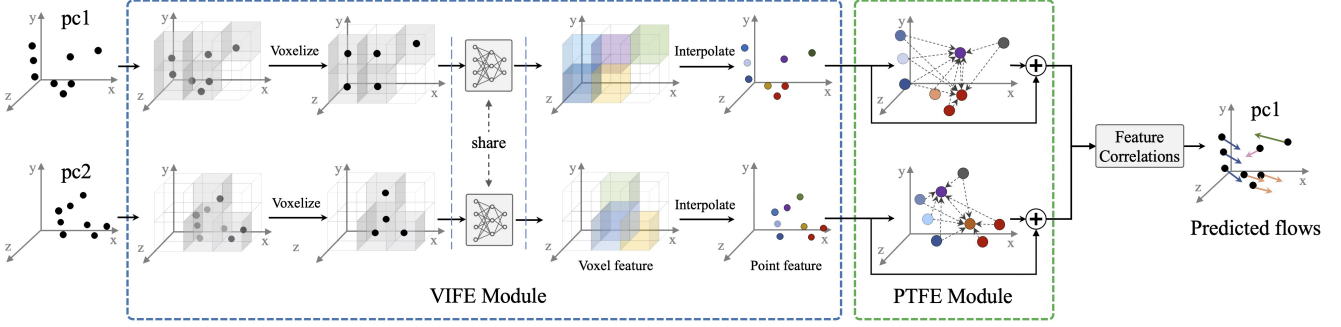


Figure 2. Overall framework of our SCTN approach. Given two consecutive point clouds, the Voxelization-Interpolation Feature Extraction (VIFE) extracts features from voxelized point clouds and then projects back the voxel features into point features. These point features are fed into the Point Transformer Feature Extraction (PTFE) module to explicitly learn point relations. With fused features of VIFE and PTFE module, SCTN computes point correlations between the point clouds and predicts flows.

Net [49], PointPWC [65] estimates scene flow in a coarse-to-fine fashion, introducing cost volume, upsampling, and warping modules for the point cloud processing. The most related recent work to our approach is FLOT [40]. FLOT addresses the scene flow as a matching problem between corresponding points in the consecutive clouds and solve it using optimal transport. Our method differs from FLOT [40] in two aspects. First, our method explicitly explores more suitable feature representation that facilitate the scene flow estimation. Second, our method is trained to enforce the consistency of predicted flows for local-region points from the same object, which is ignored in FLOT [40]. Recently, Gojcic *et al.* [14] explore weakly supervised learning for scene flow estimation using labels of ego motions as well as ground-truth foreground and background masks. Other works [26, 36, 65] study unsupervised/self-supervised learning for scene flow estimation on point clouds, proposing regularization losses that enforces local spatial smoothness of predicted flows. These losses are directly constraining points in a local region to have similar flows, but are not feature-aware.

3D Deep Learning. Many works have introduced deep representation for point cloud classification and segmentation [18, 27, 29, 31, 42, 53, 64, 69, 71]. Qi *et al.* [41] propose PointNet that learns point feature only from point positions. PointNet++ [42] extends PointNet by aggregating information from local regions. Motivated by PointNet++, many works [27, 29, 53, 69] design various local aggregation functions for point cloud classification and segmentation. Different from these point-based convolutions, [59, 66] transform point cloud into voxels, such that typical 3D convolution can be applied. However, such voxel-based convolution suffers from expensive computational and memory cost as well as information loss during voxelization. Liu *et al.* [32] combine PointNet [41] with voxel-based convolution to reduce the memory consumption. For the sake of efficient learning, researchers have explored sparse convolution for

point cloud segmentation [8, 67] which shows impressive performance. Tang *et al.* [50] propose to combine PointNet with sparse convolution for large-scale point cloud segmentation. Differently, we not only leverage voxelization and interpolation for feature extraction, but also explicitly model point relations to provide complementary information.

3. Methodology

Problem Definition. Given two consecutive point clouds \mathcal{P}^t and \mathcal{P}^{t+1} , scene flow estimation is to predict the 3D motion flow of each point from \mathcal{P}^t to \mathcal{P}^{t+1} . Let p_i^t be the 3D coordinates of i -th point in $\mathcal{P}^t = \{p_i^t\}_{i=1}^{n_p}$. Like previous work [40], we predict scene flow based on the correlations of each point pair between \mathcal{P}^t and \mathcal{P}^{t+1} . Given a pair of points $p_i^t \in \mathcal{P}^t$ and $p_j^{t+1} \in \mathcal{P}^{t+1}$, the correlation of the two points is computed as follows:

$$C(p_i^t, p_j^{t+1}) = \frac{(\mathbf{F}_i^t)^T \cdot \mathbf{F}_j^{t+1}}{\|\mathbf{F}_i^t\|_2 \|\mathbf{F}_j^{t+1}\|_2} \quad (1)$$

where \mathbf{F}_j^{t+1} is the feature of p_j^{t+1} , and $\|\cdot\|_2$ is the L2 norm.

Point feature \mathbf{F} is the key to computing the correlation $C(p_i^t, p_j^{t+1})$ which further plays an important role in scene flow estimation. Hence, it is desirable to extract effective point features that enable point pairs in corresponding regions to achieve higher correlation values between \mathcal{P}^t and \mathcal{P}^{t+1} . However, different from point cloud segmentation and classification that focus on static point cloud, scene flow estimation operates on dynamic ones, which poses new challenges for feature extraction in two aspects. For example, the input point clouds of scene flow are not only irregular and unordered, but also its density is spatially non-uniform and temporally varying, as discussed in previous sections.

Our goal is to extract locally consistent while discriminative features for points, so as to achieve accurate flow es-

timization. Different from exiting methods directly extracting point feature from the neighborhood in original point cloud, we proposed two feature extraction modules for scene flow estimation. The Voxelization-Interpolation based Feature Extraction (VIFE) is proposed to address the issue of point cloud’s non-uniform density. With the features extracted by VIFE, Point Transformer based Feature Extraction (PTFE) further enhance feature discriminability by modeling point relations globally. Since the two kinds of features provide complementary information, we fuse these features, such that the fused features provide proper correspondences to predict accurate scene flows.

Overview. Figure 2 illustrates the overall framework of our approach, that takes two consecutive point clouds \mathcal{P}^t and \mathcal{P}^{t+1} as inputs and predict the scene flow from \mathcal{P}^t to \mathcal{P}^{t+1} . First, the VIFE module extracts features for voxel points from voxelized point clouds, and projects back the voxel features into the original 3D points to obtain locally consistent point features. Second, our PTFE module improves the point feature representation by modeling relation between points. Third, with features extracted by VIFE and PTFE module, we calculate the correlations of points between \mathcal{P}^t and \mathcal{P}^{t+1} , where a sinkhorn algorithm [7, 9, 40] is leveraged to predict the flows. We train our method with an extra regularizing loss to enforce spatial consistency of predicted flows.

3.1. Voxelization-Interpolation based feature extraction

As mentioned in previous sections, the density of consecutive point clouds is spatially non-uniform and temporally varying, posing difficulties in feature extraction. To address the issue, we propose the Voxelization-Interpolation based Feature Extraction (VIFE) module. VIFE first voxelizes the consecutive point clouds into voxels. As illustrated in Figure 2, the spatial non-uniform distributions and temporally variations of points are reduced to some extent.

After that, VIFE conducts convolutions on voxel points rather than all points of the point cloud, and then interpolate features for each point. We argue that such simple operators *i.e.* voxelization and interpolation, ensure points in a local neighborhood to have smoother features, ideally leading to consistent flows in space.

Voxel feature extraction. We then leverage a U-Net [46] architecture network to extract feature from voxelized point clouds, where convolution can be many types of point cloud convolutions such as pointnet++ used in FLOT [40]. Here, we adopt sparse convolution *e.g.* Minkowski Engine [8] for efficiency. More details are available in our supplementary material.

Point feature interpolation. We project back the voxel features into point feature \mathbf{F}_i^S for point p_i . In particular, we interpolate the point features from the K closest voxels fol-

lowing equation (2). $\mathcal{N}^v(p_i)$ represents the set of K nearest neighboring non-empty voxels for the point p_i , $\mathbf{v}_k \in \mathbb{R}^C$ represents the feature of k -th closest non-empty voxel and d_{ik} the Euclidian distance between the point p_i and the center of the k -th closest non-empty voxel.

$$\mathbf{F}_i^S = \frac{\sum_{k \in \mathcal{N}^v(p_i)} d_{ik}^{-1} \cdot \mathbf{v}_k}{\sum_{k \in \mathcal{N}^v(p_i)} d_{ik}^{-1}} \quad (2)$$

We observed that close points are encouraged to have similar features, which helps our method generate consistent flows for these points. This is favorable for local object parts or rigid objects with dense densities and consistent flows (*e.g.* LiDAR points on a car at close range).

3.2. Point transformer based feature extraction

Our VIFE module adopt aggressive downsampling to obtain a large receptive field and low computation cost. However, aggressive downsampling inevitably loses some important information [50]. In such case, the features of points with large information loss are disadvantageous for estimating their scene flow. To address this issue, we explicitly exploit point relations as a complementary information on top of the point feature extracted with VIFE. Recent work [3, 70, 72] employ transformer and self-attention to model internal relation in the features, achieving impressive performance in image tasks such as detection and recognition. Similar trend appeared in point cloud classification and segmentation [12, 16, 71] showing the effectiveness of transformer in 3D. Inspired by these work, we resort to transformer for capturing point relation information as the point feature.

In an autonomous navigation scenario, point clouds represent complete scenes, with small object such as cars and trucks, but also large structure such as buildings and walls. The scene flows in such a large scene do not only depend on the aggregation from a small region, but rather a large one. As a results, we refrain in building a transformer for the local neighborhood as it would restrict the receptive field or require deeper model (*i.e.* increase the memory). Instead, our transformer module learns the relation of each point to all other points, such that the transformer can adaptively capture the rich contextual information from a complete scene.

Formally, given a point p_i , we consider every points in \mathcal{P} as query and key elements. Our transformer module builds a point feature representation for p_i by adaptively aggregating the features of all points based on self-attention:

$$\mathbf{F}_i^R = \sum_{j=1}^{n_p} A_{i,j} \cdot g_v(\mathbf{F}_j^S, \mathbf{G}_j) \quad (3)$$

where g_v is the a learnable function (*e.g.* linear function), $A_{i,j}$ is an attention defining a weight of p_j to p_i , \mathbf{G}_j is the

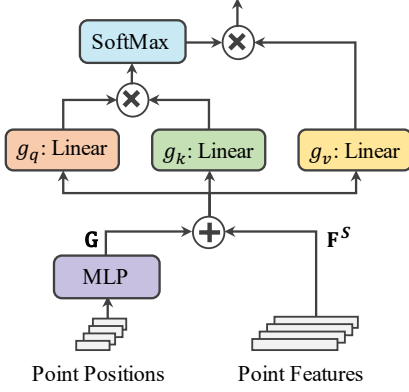


Figure 3. Details of our point transformer based feature extraction module (PTFE). \otimes and \oplus correspond to matrix multiplication and addition operations, respectively.

positional encoding feature of p_j .

As pointed in literature [3, 70], the positional encoding feature can provide important information for the transformer. The position encoding in recent transformer work [71] encodes the *relative* point position to neighbors for point cloud classification or segmentation. Different from those tasks, the task of scene flow is to find correspondences between consecutive point clouds. Thus, we argue that an *absolute* position provides sufficient information to estimate the scene flow. Therefore, given a point p , our position encoding function encodes its *absolute* position p_j :

$$\mathbf{G}_j = \phi(p_j) \quad (4)$$

where ϕ is a MLP layer. Using absolute positions reduce computational cost, compared with using relative positions.

We calculate an attention $A_{i,j}$ as the similarity between the features of p_i and p_j in an embedding space. The similarity is estimated using features and position information:

$$A_{i,j} \propto \exp\left(\frac{(g_q(\mathbf{F}_i^S, \mathbf{G}_i))^T \cdot g_k(\mathbf{F}_j^S, \mathbf{G}_j)}{c_a}\right) \quad (5)$$

where $g_q(\cdot, \cdot)$ and $g_k(\cdot, \cdot)$ are the learnable mapping functions to project feature into an embedding space, and c_a is the output dimension of $g_q(\cdot, \cdot)$ or $g_k(\cdot, \cdot)$. $A_{i,j}$ is further normalized such that $\sum_j A_{i,j} = 1$. The architecture of our transformer module is illustrated in Figure 3.

3.3. Flow prediction

Since the point feature from our VIFE and PTFE modules provide complementary information, we fuse the two kinds of features through skip connection for each point, *i.e.* $\mathbf{F}_i = \mathbf{F}_i^S + \mathbf{F}_i^R$. By feeding the fused point features into Eq. 1, we compute the correlations of all pairs $\mathbf{C}(\mathcal{P}^t, \mathcal{P}^{t+1}) = \{C(p_i^t, p_j^{t+1})\}$ between the two consecutive point clouds.

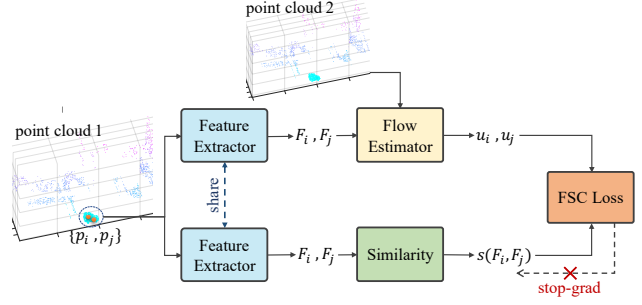


Figure 4. Stop gradient for the FSC loss. We extract the flow from a neighboring point as well as the similarity between their features. We optimize the FSC loss without back-propagating the gradients to the features from the similarity branch to avoid degenerate cases.

With the estimated point correlations, we adopt the Sinkhorn algorithm to estimate soft correspondences and predict flows for \mathcal{P}^t , following FLOT.

3.4. Training losses

We train our model to regress the scene flow in a supervised fashion, on top of which we propose a Feature-aware Spatial Consistency loss, named ‘‘FSC loss’’, that enforces similar features to have similar flow. The FSC loss provides a better generalization and transfer capability between the training and testing datasets.

Supervised loss. We define in Equation (6) our supervised loss E^s that minimize the L_1 -norm difference between the estimated flow and the ground truth flow for the non-occluded points. \mathbf{u}_i^* and \mathbf{u}_i are respectively the ground-truth and predicted motion flow for the point $p_i \in \mathcal{P}$ and m_i is a binary indicator for the non-occlusion of this point, *i.e.* $m_i = 0$ if p_i is occluded, otherwise $m_i = 1$.

$$E^s = \sum_i^N m_i \|\mathbf{u}_i - \mathbf{u}_i^*\| \quad (6)$$

Feature-aware Spatial Consistency (FSC) loss. Given a local region, points from the same object usually has consistent motions, resulting in similar flows. To model such phenomena, we propose a consistency loss that ensures points within an object/local object part to have similar predicted flows. Yet, object annotations are not necessarily available. Instead, we propose to control flow consistency according to feature similarity. That is, given a local region, if two points are of larger feature similarity, they are of the higher probability that belongs to the same object. In particular, given a point p_i with predicted flow \mathbf{u}_i and its local neighborhood $\mathcal{N}(p_i)$, we enforce the flow \mathbf{u}_j of $p_j \in \mathcal{N}(p_i)$ to be similar to \mathbf{u}_i , if the feature \mathbf{F}_i of p_i is similar to \mathbf{F}_j of

p_j . Formally, we define the FSC loss as follows:

$$E^c = \sum_{i=1}^N \frac{1}{K} \sum_{p_j \in \mathcal{N}(p_i)} s(\mathbf{F}_i, \mathbf{F}_j) \cdot \|\mathbf{u}_i - \mathbf{u}_j\|_2 \quad (7)$$

where the similarity function $s(\mathbf{F}_i, \mathbf{F}_j)$ of p_i and p_j is defined as $1 - \exp(-(\mathbf{F}_i)^T \cdot \mathbf{F}_j / \tau)$ with τ being a temperature hyper-parameter, K is the number of points in $\mathcal{N}(p_i)$.

A naive implementation of the FSC loss would inevitably lead to degenerate cases. In particular, the FSC loss is a product of two objectives: (i) a similarity $s(\mathbf{F}_i, \mathbf{F}_j)$ between the features \mathbf{F}_i and \mathbf{F}_j and (ii) a difference $\|\mathbf{u}_i - \mathbf{u}_j\|_1$ between their flows. The scope of this loss is to train the flows to be similar if they have similar features. However, to minimize the FSC loss, the model would make the features \mathbf{F}_j and \mathbf{F}_i be orthogonal (*i.e.* $\mathbf{F}_j \cdot \mathbf{F}_i = 0$), such that $s(\mathbf{F}_j, \mathbf{F}_i) = 0$ (*i.e.* $E^c = 0$). Obviously, it is against our aim.

To circumvent this limitation, we propose a stop-gradient for the FSC loss, taking inspiration from recent advances in self-supervised learning [5]. As illustrated in Figure 4, our architecture stops the propagation of the gradient in the branch extracting the feature similarity. By such architecture, our FSC loss avoids optimizing the features, while optimizing solely the flows similarities $\|\mathbf{u}_j - \mathbf{u}_i\|_1$ for neighboring points with similar features.

4. Experiments

Dataset. We conduct our experiments on two datasets that are widely used to evaluate scene flow. *FlyingThings3D* [37] is a large-scale synthetic stereo video datasets, where synthetic objects are selected from ShapeNet [4] and randomly assigned various motions. We generate 3D point clouds and ground truth scene flows with their associated camera parameters and disparities. Following the same preprocessing as in [15, 40, 65], we randomly sample 8192 points and remove points with camera depth greater than 35 m. We use the same 19640/3824 pairs of point cloud (training/testing) used in the related works [15, 40, 65]. *KITTI Scene Flow* [8, 35] is a real-world Lidar scan dataset for scene flow estimation from the KITTI autonomous navigation suite. Following the preprocessing of [15], we leverage 142 point cloud pairs of 8192 points for testing. For a fair comparison, we also remove ground points by discarding points whose height is lower than -1.4 m, following the setting of existing methods [15, 40, 65].

Evaluation Metrics. To evaluate the performance of our approach, we adopt the standard evaluation metrics used in the related methods [40, 65], described as follows: The *EPE3D* (m) (3D end-point-error) is calculated by computing the average L_2 distance between the predicted and GT scene flow, in meters. This is our main metric. The *Acc3DS*

is a strict version of the accuracy which estimated as the ratio of points whose *EPE3D* < 0.05 m or relative error $< 5\%$. The *Acc3DR* is a relaxed accuracy which is calculated as the ratio of points whose *EPE3D* < 0.10 m or relative error $< 10\%$. The *Outliers* is the ratio of points whose *EPE3D* > 0.30 m or relative error $> 10\%$.

Implementation Details. We implement our method in PyTorch [39]. We train our method on FlyingThing3D then evaluate on FlyingThing3D and KITTI. We minimize a cumulative loss $E = E^s + \lambda E^c$ with $\lambda = 0.30$ a weight that scale the losses. We use the Adam optimizer [25] with an initial learning rate of 10^{-3} , which is dropped to 10^{-4} after the 50^{th} epoch. First, we train for 40 epochs only using the supervised loss. Then we continue the training for 20 epochs with both the supervision loss and the FSC loss, for a total on 60 epochs. We use a voxel size of resolution 0.07m.

Runtime. We evaluate the running time of our method. Table 3 reports the evaluated time compared with recent state-of-the-art methods. FLOT [40] is the most related work to our method, since we both adopt point-wise correlations to generate predicted flows. Our method consumes lower running time than FLOT, although the transformer module is equipped.

4.1. Quantitative Evaluation

We compare our approach with recent deep-learning-based methods including FlowNet3D [30], HPLFlowNet [15], PointPWC [65] and FLOT [40]. These methods are state-of-the-art in scene flow estimation from point cloud data and do not leverage any additional labels such as ground-truth ego motions or instance segmentation.

Results on FlyingThings3D. We train and evaluate our model on the FlyThings3D datasets. As shown in Table 1, our method outperforms all methods in every metrics by a significant margin. It is worth noting that our method obtains an *EPE3D* metric below 4cm, with a relative improvement of 26.9% and 35.5% over the most recent methods FLOT [40] and PointPWC [65], respectively. The performance shows that our method is effective in predicting flows with high accuracy.

Results on KITTI without Fine-tune. Following the common practice [40, 65], we train our model on FlyingThings3D and directly test the trained model on KITTI Scene Flow dataset, without any fine-tuning, to evaluate the generalization capability of our method. We report in Table 1 the highest accuracy of scene flow estimation on KITTI Scene Flow dataset for our SCTN method. Again, we reduce the *EPE3D* metric below 4cm, with a 33.9% relative improvement over FLOT [40]. In the *Acc3DS* metrics, our method outperforms both FLOT [40] and PointPWC [65] by 13.5% and 16.6% respectively. This results highlight the capability of our method to generalize well on real-world point cloud

Dataset	Method	EPE3D(m) ↓	Acc3DS ↑	Acc3DR ↑	Outliers ↓
FlyingThings3D	FlowNet3D [30]	0.114	0.412	0.771	0.602
	HPLFlowNet [15]	0.080	0.614	0.855	0.429
	PointPWC [65]	0.059	0.738	0.928	0.342
	EgoFlow [54]	0.069	0.670	0.879	0.404
	FLOT [40]	0.052	0.732	0.927	0.357
	SCTN (ours)	0.038	0.847	0.968	0.268
KITTI	FlowNet3D [30]	0.177	0.374	0.668	0.527
	HPLFlowNet [15]	0.117	0.478	0.778	0.410
	PointPWC [65]	0.069	0.728	0.888	0.265
	EgoFlow [54]	0.103	0.488	0.822	0.394
	FLOT [40]	0.056	0.755	0.908	0.242
	SCTN (ours)	0.037	0.873	0.959	0.179

Table 1. Comparison with the state-of-the-art on FlyingThings3D and KITTI. Best results in bold. Our proposed model SCTN reaches highest performances in all metrics.

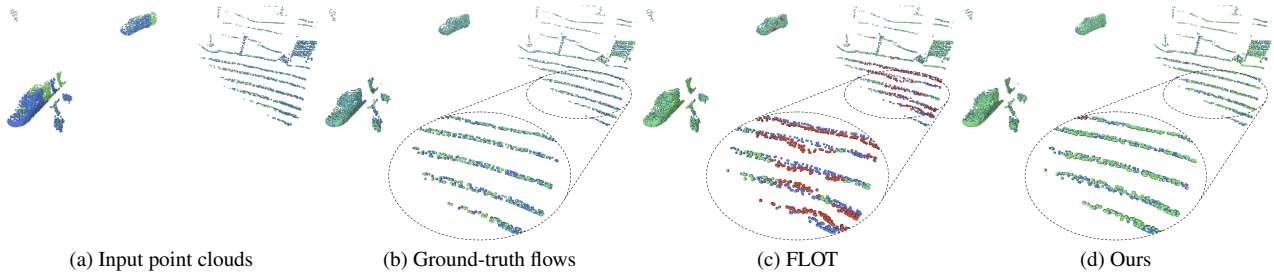


Figure 5. Qualitative comparison results. Green points indicate the first point cloud in (a), and blue points indicate the second point cloud in (a)(b)(c)(d). In (b)(c)(d), green points are the ones in the first point cloud warped by correctly predicted flows, while red points are the ones warped by incorrect flows (the first point cloud + incorrect scene flow whose EPE3D > 0.1m).

VIFE	PTFE	FSC loss	EPE3D(m) ↓	Acc3DS ↑
✓			0.045	0.835
✓		✓	0.042	0.853
✓	✓		0.040	0.863
✓	✓	✓	0.037	0.873

Table 2. Ablation for SCTN. We further analyse the performances of our three components: VIFE, PTFE and FSC loss on KITTI. We highlight in bold the best performances.

dataset.

4.2. Qualitative Evaluation

To qualitatively evaluate the quality of our scene flow predictions, we visualize the predicted scene flow and ground-truth one in Figure 5. Since FLOT [40] is most related to our method, we compare the qualitative performances of our SCTN with FLOT [40].

Points in a local region from the same object usually have similar ground-truth flows. Yet, FLOT introduces prediction errors in local regions, highlighting the inconsistency in the scene flow predictions. For example, FLOT

Method	Runtime (ms)
FLOT [40]	389.3
SCTN (ours)	242.7

Table 3. Running time comparisons. The runtime of FLOT and our SCTN are evaluated on a single GTX2080Ti GPU. We used the official implementation of FLOT.

inaccurately predicts scene flow for some regions in the background, even though those points have similar flows, as shown in Figure 5. In contrast, our method is more consistent in the prediction for points in the same object, achieving better performance, *e.g.* for the background objects with complex structure.

4.3. Ablation Study

To study the roles of the proposed VIFE, PTFE and FSC loss, we ablate each proposed component of our model and evaluate their performance on KITTI datasets. For all the experiments, we follow the same training procedure than in the main results. Table 2 reports the evaluation results.

VIFE module. Table 2 shows that our approach with

the sole VIEF convolution module already outperforms the state-of-the-art methods listed in Table 1. Different from existing methods directly applying convolution on original point clouds, our VIFE extracts feature from voxelized point cloud, which reduces the non-uniform density of point cloud, while ensuring that points in a local region have consistent features, to some extent. The results show that such features are favorable for scene flow estimation.

PTFE module. Compared with only using VIFE module, adding PTFE improves metrics on KITTI as reported in the third row in Table 2. For example, EPE3D is improved by 11.1%, compared with only using the VIEF module. Our PIFE module explicitly learns point relations, which provides rich contextual information and helps to match corresponding points even for objects with complex structures.

FSC loss. Table 2 shows that adding the FSC loss helps to achieve better scene flow estimation on KITTI. Our FSC loss improves the generalization capability of our method.

5. Conclusion

We present a Sparse Convolution-Transformer Network (SCTN) for scene flow estimation. Our SCTN leverages the VIFE module to transfer irregular point cloud into locally smooth flow features for estimating spatially consistent motions in local regions. Our PTFE module learns rich contextual information via explicitly modeling point relations, which is helpful for matching corresponding points and benefits scene flow estimation. A novel FSC loss is also proposed for training SCTN, improving the generalization ability of our method. Our approach achieves state-of-the-art performances on FlyingThings3D and KITTI datasets.

6. Acknowledgments

This work was supported by the King Abdullah University of Science and Technology (KAUST) Office of Sponsored Research through the Visual Computing Center (VCC) funding. We thank Hani Itani for his constructive suggestions and help.

References

- [1] Michael J Black and Padmanabhan Anandan. A framework for the robust estimation of optical flow. In *ICCV*, pages 231–236. IEEE, 1993. 2
- [2] Thomas Brox, Christoph Bregler, and Jitendra Malik. Large displacement optical flow. In *CVPR*, pages 41–48. IEEE, 2009. 2
- [3] Nicolas Carion, Francisco Massa, Gabriel Synnaeve, Nicolas Usunier, Alexander Kirillov, and Sergey Zagoruyko. End-to-end object detection with transformers. In *ECCV*, pages 213–229, 2020. 2, 4, 5
- [4] Angel X. Chang, Thomas Funkhouser, Leonidas Guibas, Pat Hanrahan, Qixing Huang, Zimo Li, Silvio Savarese, Manolis Savva, Shuran Song, Hao Su, Jianxiong Xiao, Li Yi, and Fisher Yu. ShapeNet: An information-rich 3D model repository. Technical Report arXiv:1512.03012 [cs.GR], arXiv preprint, 2015. 6
- [5] Xinlei Chen and Kaiming He. Exploring simple siamese representation learning, 2020. 6
- [6] Yuhua Chen, Luc Van Gool, Cordelia Schmid, and Cristian Sminchisescu. Consistency guided scene flow estimation. In *ECCV*, pages 125–141. Springer, 2020. 2
- [7] Lenaïc Chizat, Gabriel Peyré, Bernhard Schmitzer, and François-Xavier Vialard. Scaling algorithms for unbalanced optimal transport problems. *Mathematics of Computation*, 87(314):2563–2609, 2018. 4
- [8] Christopher Choy, JunYoung Gwak, and vito Savarese. 4d spatio-temporal convnets: Minkowski convolutional neural networks. In *CVPR*, pages 3075–3084, 2019. 3, 4, 6
- [9] Marco Cuturi. Sinkhorn distances: lightspeed computation of optimal transport. In *NeurIPS*, volume 2, page 4, 2013. 4
- [10] Ayush Dewan, Tim Caselitz, Gian Diego Tipaldi, and Wolfram Burgard. Rigid scene flow for 3d lidar scans. In *IROS*, pages 1765–1770. IEEE, 2016. 2
- [11] Alexey Dosovitskiy, Philipp Fischer, Eddy Ilg, Philip Hausser, Caner Hazirbas, Vladimir Golkov, Patrick Van Der Smagt, Daniel Cremers, and Thomas Brox. FlowNet: Learning optical flow with convolutional networks. In *ICCV*, pages 2758–2766, 2015. 2
- [12] Nico Engel, Vasileios Belagiannis, and Klaus Dietmayer. Point transformer, 2020. 4
- [13] Andreas Geiger, Philip Lenz, Christoph Stiller, and Raquel Urtasun. Vision meets robotics: The kitti dataset. *The International Journal of Robotics Research*, 32(11):1231–1237, 2013. 1
- [14] Zan Gojcic, Or Litany, Andreas Wieser, Leonidas J. Guibas, and Tolga Birdal. Weakly supervised learning of rigid 3d scene flow. In *CVPR*, pages 5692–5703, June 2021. 3
- [15] Xiuye Gu, Yijie Wang, Chongruo Wu, Yong Jae Lee, and Panqu Wang. HplflowNet: Hierarchical permutohedral lattice flowNet for scene flow estimation on large-scale point clouds. In *CVPR*, 2019. 2, 6, 7
- [16] Meng-Hao Guo, Jun-Xiong Cai, Zheng-Ning Liu, Tai-Jiang Mu, Ralph R. Martin, and Shi-Min Hu. Pct: Point cloud transformer, 2021. 4
- [17] Berthold KP Horn and Brian G Schunck. Determining optical flow. *Artificial intelligence*, 17(1-3):185–203, 1981. 2
- [18] Wei Hu, Jiahao Pang, Xianming Liu, Dong Tian, Lin Chia-Wen, and Vetro Anthony. Graph signal processing for geometric data and beyond: Theory and applications. *IEEE Trans. Multimedia*, 2022. 3
- [19] Frédéric Huguet and Frédéric Devernay. A variational method for scene flow estimation from stereo sequences. In *ICCV*, pages 1–7. IEEE, 2007. 2
- [20] Tak-Wai Hui and Chen Change Loy. LiteflowNet3: Resolving correspondence ambiguity for more accurate optical flow estimation. In *ECCV*, pages 169–184. Springer, 2020. 2
- [21] Tak-Wai Hui, Xiaoou Tang, and Chen Change Loy. LiteflowNet: A lightweight convolutional neural network for optical flow estimation. In *CVPR*, pages 8981–8989, 2018. 2

- [22] Eddy Ilg, Nikolaus Mayer, Tonmoy Saikia, Margret Keuper, Alexey Dosovitskiy, and Thomas Brox. FlowNet 2.0: Evolution of optical flow estimation with deep networks. In *CVPR*, pages 2462–2470, 2017. 2
- [23] Eddy Ilg, Tonmoy Saikia, Margret Keuper, and Thomas Brox. Occlusions, motion and depth boundaries with a generic network for disparity, optical flow or scene flow estimation. In *ECCV*, pages 614–630, 2018. 2
- [24] Huaizu Jiang, Deqing Sun, Varun Jampani, Zhaoyang Lv, Erik Learned-Miller, and Jan Kautz. Sense: A shared encoder network for scene-flow estimation. In *ICCV*, pages 3195–3204, 2019. 2
- [25] Diederik P Kingma and Jimmy Ba. Adam: A method for stochastic optimization. *arXiv preprint arXiv:1412.6980*, 2014. 6
- [26] Yair Kittenplon, Yonina C. Eldar, and Dan Raviv. Flow-step3d: Model unrolling for self-supervised scene flow estimation. In *CVPR*, pages 4114–4123, June 2021. 3
- [27] Huan Lei, Naveed Akhtar, and Ajmal Mian. Spherical kernel for efficient graph convolution on 3d point clouds. *TPAMI*, 2020. 3
- [28] Ruibo Li, Guosheng Lin, Tong He, Fayao Liu, and Chunhua Shen. Hcrf-flow: Scene flow from point clouds with continuous high-order crfs and position-aware flow embedding. In *Proceedings of the IEEE/CVF Conference on Computer Vision and Pattern Recognition (CVPR)*, pages 364–373, June 2021. 1
- [29] Yangyan Li, Rui Bu, Mingchao Sun, Wei Wu, Xinhan Di, and Baoquan Chen. Pointcnn: Convolution on χ -transformed points. In *NeurIPS*, pages 828–838, 2018. 3
- [30] Xingyu Liu, Charles R Qi, and Leonidas J Guibas. FlowNet3d: Learning scene flow in 3d point clouds. In *CVPR*, 2019. 1, 2, 6, 7
- [31] Ze Liu, Han Hu, Yue Cao, Zheng Zhang, and Xin Tong. A closer look at local aggregation operators in point cloud analysis. In *ECCV*, pages 326–342. Springer, 2020. 3
- [32] Zhijian Liu, Haotian Tang, Yujun Lin, and Song Han. Point-voxel cnn for efficient 3d deep learning. In *NeurIPS*, 2019. 3
- [33] Wei-Chiu Ma, Shenlong Wang, Rui Hu, Yuwen Xiong, and Raquel Urtasun. Deep rigid instance scene flow. In *CVPR*, 2019. 2
- [34] Nikolaus Mayer, Eddy Ilg, Philip Häusser, Philipp Fischer, Daniel Cremers, Alexey Dosovitskiy, and Thomas Brox. A large dataset to train convolutional networks for disparity, optical flow, and scene flow estimation. In *CVPR*, pages 4040–4048, 2016. 2
- [35] Moritz Menze, Christian Heipke, and Andreas Geiger. Object scene flow. *JPRS*, 2018. 2, 6
- [36] Himangi Mittal, Brian Okorn, and David Held. Just go with the flow: Self-supervised scene flow estimation. In *CVPR*, June 2020. 3
- [37] N.Mayer, E.Ilg, P.Häusser, P.Fischer, D.Cremers, A.Dosovitskiy, and T.Brox. A large dataset to train convolutional networks for disparity, optical flow, and scene flow estimation. In *CVPR*, 2016. 2, 6
- [38] N.Mayer, E.Ilg, P.Häusser, P.Fischer, D.Cremers, A.Dosovitskiy, and T.Brox. A large dataset to train convolutional networks for disparity, optical flow, and scene flow estimation. In *CVPR*, 2016. 2
- [39] Adam Paszke, Sam Gross, Francisco Massa, Adam Lerer, James Bradbury, Gregory Chanan, Trevor Killeen, Zeming Lin, Natalia Gimelshein, Luca Antiga, et al. Pytorch: An imperative style, high-performance deep learning library. *arXiv preprint arXiv:1912.01703*, 2019. 6
- [40] Gilles Puy, Alexandre Boulch, and Renaud Marlet. FLOT: Scene Flow on Point Clouds Guided by Optimal Transport. In *ECCV*, 2020. 1, 2, 3, 4, 6, 7, 11, 12, 13, 14
- [41] Charles R Qi, Hao Su, Kaichun Mo, and Leonidas J Guibas. PointNet: Deep learning on point sets for 3d classification and segmentation. In *CVPR*, pages 652–660, 2017. 3
- [42] Charles R Qi, Li Yi, Hao Su, and Leonidas J Guibas. PointNet++: Deep hierarchical feature learning on point sets in a metric space. In *NeurIPS*, pages 5099–5108, 2017. 2, 3
- [43] Haozhe Qi, Chen Feng, Zhiguo Cao, Feng Zhao, and Yang Xiao. P2b: Point-to-box network for 3d object tracking in point clouds. In *CVPR*, pages 6329–6338, 2020. 1
- [44] Julian Quiroga, Thomas Brox, Frédéric Devernay, and James Crowley. Dense semi-rigid scene flow estimation from rgbd images. In *ECCV*, pages 567–582. Springer, 2014. 2
- [45] René Ranftl, Kristian Bredies, and Thomas Pock. Non-local total generalized variation for optical flow estimation. In *ECCV*, pages 439–454. Springer, 2014. 2
- [46] Olaf Ronneberger, Philipp Fischer, and Thomas Brox. U-net: Convolutional networks for biomedical image segmentation. In *MICCAI*, pages 234–241. Springer, 2015. 4
- [47] Shaoshuai Shi, Chaoxu Guo, Li Jiang, Zhe Wang, Jianping Shi, Xiaogang Wang, and Hongsheng Li. Pv-rcnn: Point-voxel feature set abstraction for 3d object detection. In *CVPR*, pages 10529–10538, 2020. 1
- [48] Deqing Sun, Erik B Sudderth, and Hanspeter Pfister. Layered rgbd scene flow estimation. In *CVPR*, pages 548–556, 2015. 2
- [49] Deqing Sun, Xiaodong Yang, Ming-Yu Liu, and Jan Kautz. Pwc-net: Cnns for optical flow using pyramid, warping, and cost volume. In *CVPR*, 2018. 2, 3
- [50] Haotian* Tang, Zhijian* Liu, Shengyu Zhao, Yujun Lin, Ji Lin, Hanrui Wang, and Song Han. Searching efficient 3d architectures with sparse point-voxel convolution. In *ECCV*, 2020. 3, 4
- [51] Zachary Teed and Jia Deng. Raft-3d: Scene flow using rigid-motion embeddings. *arXiv preprint arXiv:2012.00726*, 2020. 2
- [52] Zachary Teed and Jia Deng. Raft: Recurrent all-pairs field transforms for optical flow. In *ECCV*, pages 402–419. Springer, 2020. 2
- [53] Hugues Thomas, Charles R Qi, Jean-Emmanuel Deschaud, Beatriz Marcotegui, François Goulette, and Leonidas J Guibas. Kpconv: Flexible and deformable convolution for point clouds. In *ICCV*, pages 6411–6420, 2019. 1, 3
- [54] Ivan Tishchenko, Sandro Lombardi, Martin R Oswald, and Marc Pollefeys. Self-supervised learning of non-rigid residual flow and ego-motion. *arXiv preprint arXiv:2009.10467*, 2020. 7

- [55] Arash K Ushani, Ryan W Wolcott, Jeffrey M Walls, and Ryan M Eustice. A learning approach for real-time temporal scene flow estimation from lidar data. In *ICRA*, pages 5666–5673. IEEE, 2017. 2
- [56] Sundar Vedula, Simon Baker, Peter Rander, Robert Collins, and Takeo Kanade. Three-dimensional scene flow. In *ICCV*, volume 2, pages 722–729. IEEE, 1999. 1
- [57] Christoph Vogel, Konrad Schindler, and Stefan Roth. Piecewise rigid scene flow. In *ICCV*, pages 1377–1384, 2013. 2
- [58] Haiyan Wang, Jiahao Pang, Muhammad A. Lodhi, Yingli Tian, and Dong Tian. Festa: Flow estimation via spatial-temporal attention for scene point clouds. In *CVPR*, June 2021. 1
- [59] Peng-Shuai Wang, Yang Liu, Yu-Xiao Guo, Chun-Yu Sun, and Xin Tong. O-cnn: Octree-based convolutional neural networks for 3d shape analysis. *ACM Trans. Graph.*, 36(4):72:1–72:11, 2017. 3
- [60] Zirui Wang, Shuda Li, Henry Howard-Jenkins, Victor Prisacariu, and Min Chen. Flownet3d++: Geometric losses for deep scene flow estimation. In *WACV*, March 2020. 2
- [61] Andreas Wedel, Clemens Rabe, Tobi Vaudrey, Thomas Brox, Uwe Franke, and Daniel Cremers. Efficient dense scene flow from sparse or dense stereo data. In *ECCV*, pages 739–751. Springer, 2008. 2
- [62] Yi Wei, Ziyi Wang, Yongming Rao, Jiwen Lu, and Jie Zhou. PV-RAFT: Point-Voxel Correlation Fields for Scene Flow Estimation of Point Clouds. In *CVPR*, 2021. 1
- [63] Philippe Weinzaepfel, Jerome Revaud, Zaid Harchaoui, and Cordelia Schmid. Deepflow: Large displacement optical flow with deep matching. In *ICCV*, pages 1385–1392, 2013. 2
- [64] Wenxuan Wu, Zhongang Qi, and Li Fuxin. Pointconv: Deep convolutional networks on 3d point clouds. In *CVPR*, pages 9621–9630, 2019. 3
- [65] Wenxuan Wu, Zhi Yuan Wang, Zhuwen Li, Wei Liu, and Li Fuxin. Pointpwc-net: Cost volume on point clouds for (self-) supervised scene flow estimation. In *ECCV*, pages 88–107, 2020. 1, 2, 3, 6, 7, 11
- [66] Zhirong Wu, Shuran Song, Aditya Khosla, Fisher Yu, Linguang Zhang, Xiaoou Tang, and Jianxiong Xiao. 3d shapenets: A deep representation for volumetric shapes. In *CVPR*, pages 1912–1920, 2015. 3
- [67] Saining Xie, Jiatao Gu, Demi Guo, Charles R. Qi, Leonidas Guibas, and Or Litany. Pointcontrast: Unsupervised pre-training for 3d point cloud understanding. In *ECCV*, 2020. 3
- [68] Christopher Zach, Thomas Pock, and Horst Bischof. A duality based approach for realtime tv-l1 optical flow. In *Joint pattern recognition symposium*, pages 214–223. Springer, 2007. 2
- [69] Zhiyuan Zhang, Binh-Son Hua, and Sai-Kit Yeung. Shell-net: Efficient point cloud convolutional neural networks using concentric shells statistics. In *ICCV*, October 2019. 3
- [70] Hengshuang Zhao, Jiaya Jia, and Vladlen Koltun. Exploring self-attention for image recognition. In *CVPR*, June 2020. 4, 5
- [71] Hengshuang Zhao, Li Jiang, Jiaya Jia, Philip Torr, and Vladlen Koltun. Point transformer. In *ICCV*, 2021. 3, 4, 5
- [72] Xizhou Zhu, Weijie Su, Lewei Lu, Bin Li, Xiaogang Wang, and Jifeng Dai. Deformable detr: Deformable transformers for end-to-end object detection. In *ICLR*, 2021. 4

7. Appendix

7.1. Qualitative Results on FlyingThings3D

We provide qualitative results of our method on FlyingThings3D dataset.

Figure 6 shows three examples where point clouds are with large motions (see large position differences between orange and green point cloud in Figure 6a). FLOT introduces medium errors in large regions of objects especially in uniform regions. In contrast, our method better predicts flows, since our transformer captures rich context information for finding correspondences and FSC loss adaptively enforces flow consistency.

Figure 7 shows three examples where point clouds containing complex scene or objects with complex structure. Our method achieves better performance than FLOT. Our transformer can learn meaningful structure information via explicitly modeling point relation.

In addition, we warp the first point cloud \mathcal{P} using the predicted scene flow and visualize the warped point cloud, like FLOT [40] and PointPWC [65] did. If the warped point cloud using predicted flows is similar to that using ground-truth flows, the predicted flows are of high accurate. As shown in Figure 8, since our method predicts higher accurate flows than FLOT, the warped point cloud using our predicted flows is more similar to that using ground-truth flows.

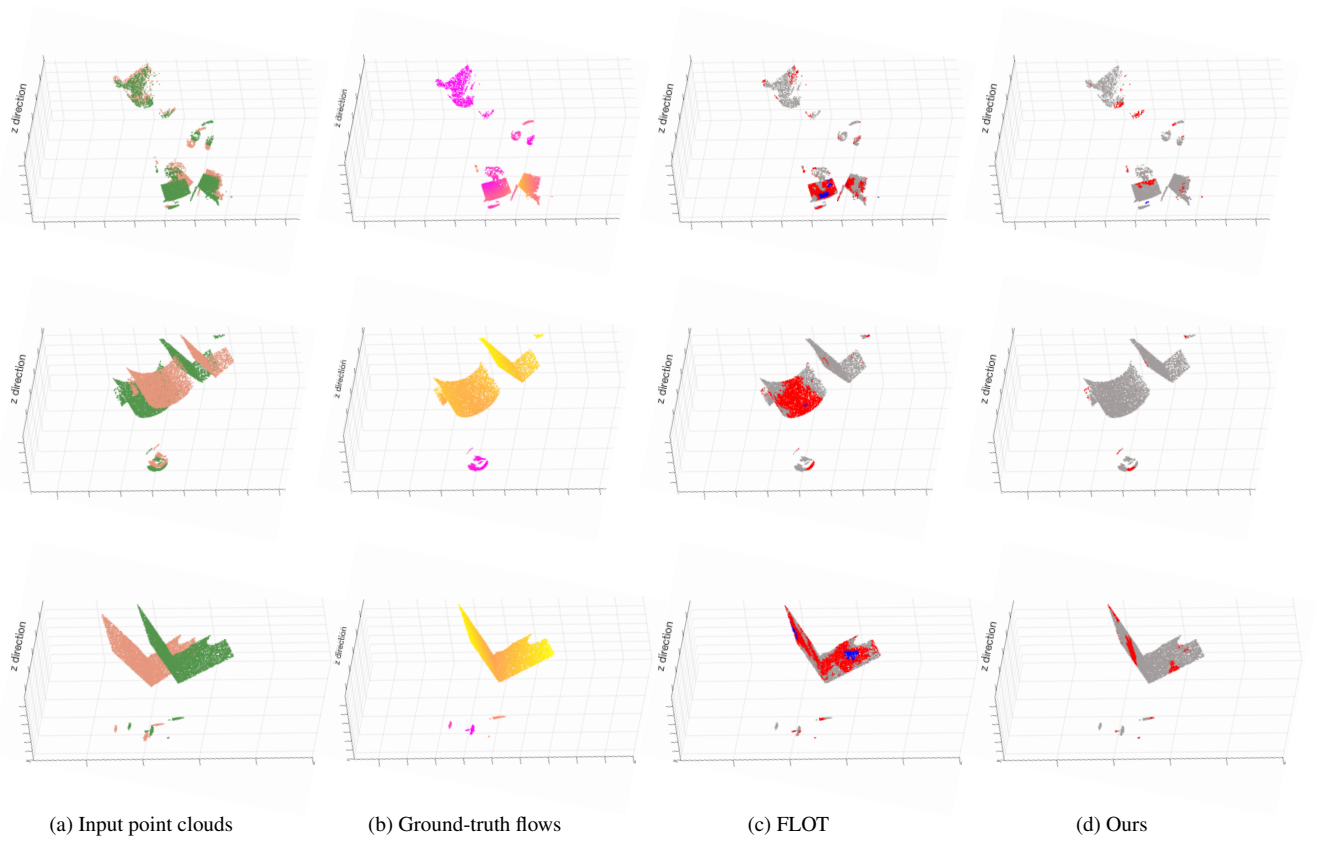


Figure 6. **Qualitative comparisons between FLOT [40] and our method on Flythings3D dataset.** Orange and green indicates the first and second point clouds in (a). The similar color indicates the point cloud has the similar flows in (b). Gray, red and blue color indicate small, medium and large errors in (c)(d).



Figure 7. **Qualitative comparisons between FLOT [40] and our method on Flythings3D dataset.** Orange and green indicates the first and second point clouds in (a). The similar color indicates the point cloud has the similar flows in (b). Gray, red and blue color indicate small, medium and large errors in (c)(d).

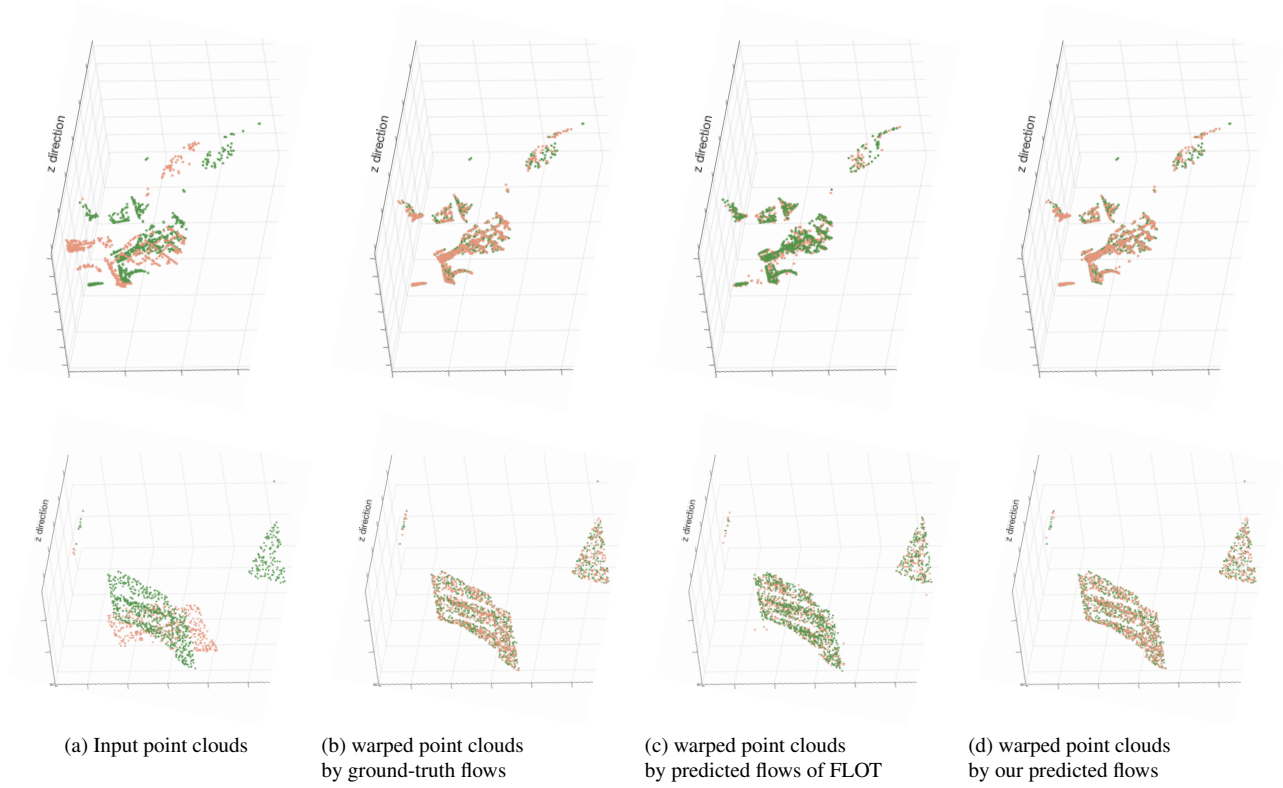


Figure 8. **Qualitative comparisons between FLOT [40] and our method on Flythings3D dataset.** Orange and green indicates the first and second point clouds in (a)(b)(c)(d). The first point cloud is warped by ground-truth flows in (b), and is warped by predicted flows of FLOT in (c) and our method in (d), respectively. Compared with FLOT, the warped first point cloud by our predicted flows is more similar to that by ground-truth flows, indicating better estimation accuracy of our method.